

# Estimate effective interaction potentials from the static structure factor in pure fluids and nanocolloids

A. Oprisan\*, S.A. Oprisan\*, A. Teklu\* and J.J. Hegseth\*\*

\*College of Charleston, 66 George Street, Charleston, SC 29424, US

\*Tel. (843) 953-7582. Fax:(843) 953-4824. Email: [oprisana@cofc.edu](mailto:oprisana@cofc.edu)

\*\*University of New Orleans, 2000 Lakeshore Drive, New Orleans, LA

## ABSTRACT

Both in critical fluids in microgravity and in nanocolloids on Earth there are long-range correlations leading to phase separation, respectively, giant concentration-driven fluctuations. Small angle light scattering is commonly used for studying fluctuations and phase separation involving structures that are in the size range up to a hundred nanometers. The static structure factor is the Fourier transformed pair correlation function, which describes the arrangement of the particles in real space. We used experimental data for pure fluids near critical point in microgravity and nanocolloids on Earth to investigate similarities between the effective interaction potentials. For this purpose, the structure factor was determined from two-dimensional snapshots of the sample cell. Using Ornstein-Zernike approximation, we directly integrated the structure factor and obtained the radial distribution function, which it is a measure of the probability of finding a particle at a distance  $r$  away from a given reference particle.

**Keywords:** near-critical fluid, nanocolloids, structure factor, radial distribution function, interaction potential

## 1 INTRODUCTION

This paper is motivated by the existing universality laws in pure fluids under microgravity conditions [1, 2] and giant concentration fluctuations induced by long-range correlations in nanocolloids [3]. Small angle scattering is one of the most important techniques for studying fluctuations and phase separation involving structures that are in the size range up to a hundred nanometers [4, 5]. Scattered light interferes with transmitted light through transparent media and gives a profile called scattered intensity as a function of scattering angle, which contains information about the configuration of the scattering centers. Among other components, the scattered intensity contains information about the particle interaction, the so-called structure factor. The (static) structure factor is the Fourier transformed pair correlation function, which describes the arrangement of the particles in real space. Fourier inversion of the structure factor gives the radial distribution function (RDF) with a spatial resolution inversely proportional to the maximum value of the scattering vector attained in the experiment. The RDF

provides information about the probability of finding an atom in a spherical shell at a distance  $r$  from an arbitrary atom. Successive peaks correspond to the nearest-, the second- and the next-neighbor atomic distribution [6, 7]. Although the structure factor is a statistical average representation of interaction potential among particles it still can be used to infer viable microscopic theoretical and computational models of nonequilibrium systems [8]. The direct visualization and analysis of critical fluctuations in pure fluids in microgravity, binary mixture, and concentration-driven interface fluctuations in nanocolloids provide invaluable information about cooperative phenomena and the role played by fluctuations in mixing, phase separation, and crystallization.

Near critical point, fluids have a very large compressibility and, therefore, they compress under their own weight and stratify due to the gravitational field. Any measurement of thermodynamic properties made on a cell of finite height in a gravitational field actually gives a macroscopic averaged property of the fluid over different densities rather than the precise property approaching the critical point. Among other advantages, experiments in microgravity eliminate the complication due to the fluid compressibility near critical point [1, 2] and allow visualization of fluctuations and phase separation processes over a significantly long duration. On Earth, nanocolloids could be used to investigate long-range correlations leading to giant concentration fluctuations [3]. Although the long-range correlations in critical fluids and nanocolloids have different sources, we are interested in investigating the similarities that might exist at the level of microscopic interaction potentials.

## 2 EXPERIMENTAL SETUP

### 2.1 Near critical fluid in microgravity

The cell containing the pure fluid consisted of a cylindrical cell made of a thin copper alloy encapsulating a layer of SF<sub>6</sub> sandwiched between two sapphire windows (Fig. 1). The geometric characteristics of the cell are as follows:  $D = 12$  mm (the diameter of the cylindrical cell),  $L = 4.34$  mm (the thickness of SF<sub>6</sub> layer), and  $\Gamma = D/L = 2.765$  (the aspect ratio of the cell). One of the advantages of using thick cell is that the phase separation can be observed for a long time and the clusters of the minority phase can grow to

a large size before wetting effects from the wall can influence them. Inside the SCU three thermistors are embedded for temperature measurement.

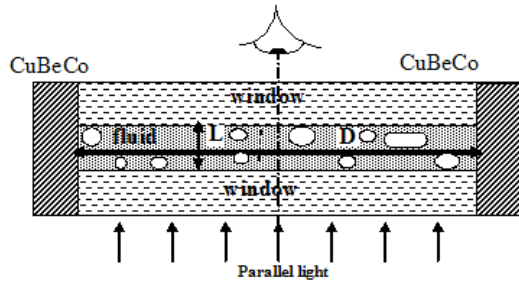


Figure 1. A schematic representation of the experimental cell (SCU) encapsulating a layer of SF<sub>6</sub> between two sapphire windows.

Another advantage of the tick cells is that they allow the three thermistors to be located away from any thermal boundary layer that may exist at the walls. The volume enclosed by the cylindrical cell contained a pure fluid (SF<sub>6</sub>) with a density close to the critical density. The cell is placed inside of a copper sample cell unit that, in turn, is placed inside a thermostat. The thermostat is designed to ensure a precise thermal control and is aligned with the optical instruments. The SCU also uses two types of thermistors, one for temperature control and the other for temperature measurement,  $T_m$ . The thermistors  $Th_1$ ,  $Th_2$ ,  $Th_3$  are located inside the cell as shown in Fig. 2C. The thermistors  $Th_1$ ,  $Th_2$ , and  $Th_3$  are all at approximately the same temperature. The measurement thermistor  $T_m$  was placed inside the SCU such that  $T_m$  represents only approximately the temperature inside the fluid phase. The results reported here for microgravity only refer to a 3.6 mK temperature quench that led to fluid separation. Near the critical point, the minority domain rapidly grows directly from the fluctuations. The density fluctuations are visualized through light transmission normal to the windows using a LED light source at 633 nm and an optical microscope of a 3.1  $\mu\text{m}$  resolution. A full description of the experimental setup is presented elsewhere [9].

## 2.2 Nanocolloids on Earth

We studied the evolution of the wavelength fluctuations in silica and gold colloids. Our optical setup of a free-diffusion experiment is schematically represented in Fig. 2. A water-soluble colloid was confined in a Hellma 120-os-20 cylindrical glass cell, 2.0 cm diameter and 2.0 cm height with plane-parallel optical glass windows [3, 10]. The interface between the two fluids was perpendicular to the gravitational field. A denser gold colloid was slowly injected using a bent needle at the bottom of the cell completely filled with degassed water. The two fluids are initially separated by a sharp horizontal interface localized almost in the middle of the diffusion cell. A parallel beam

of light from a 10 mw He-Ne laser, with a wavelength of 635.5 nm, was collimated and passed vertically upward through the diffusion cell. A progressive scan Sony CCD camera, with sensor area of 5.8 mm x 4.92 mm and a pixel resolution of 4.65  $\mu\text{m}$ , and a video lens-10x objective were used for image recording.

Gold nanocolloids with the average nanoparticles of 20 nm were used. Our results showed that the density concentration fluctuations causing local perturbation in the intensity of transmitted and scattered light cover both gravitational and diffusion effects. Using our experimental data, we were able to analyze the structure factor and their corresponding power spectra for different wave vectors and the correlation time from intermediate to late stage.

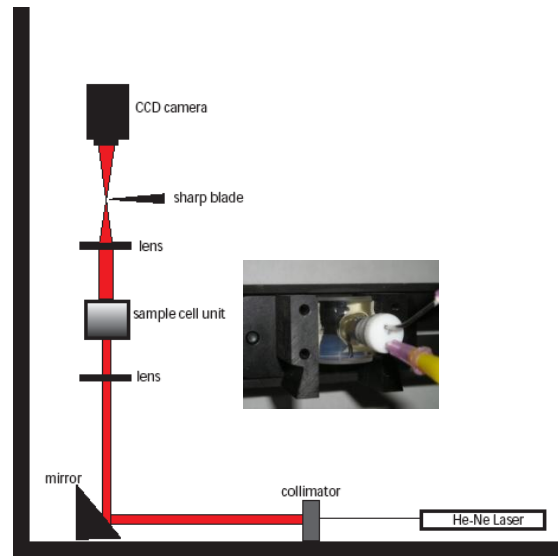


Figure 2. Schematic representation of the experimental setup (left) and a picture of the sample cell unit (right) used to study the giant fluctuations determined by diffusion in a mixture of silica (bottom) and water.

## 3 METHOD

The first milestone was to compute the **structure factor** from recorded images. Briefly, we followed this procedure:

1. Normalize recorded images in order to reduce the effect of variable light intensity. We considered both filtering [9] and averaging [10] as our starting points for image denoising.
2. Compute fluctuating image by subtracting from the normalized image a normalized background. For critical fluids, the background was given by images recorded above critical temperature. For nanocolloids, the background was recorded with the empty cell or by averaging method (static structure factor), or determined explicitly from the temporal correlations among the images (dynamic structure factor).
3. Compute the power spectrum of the fluctuation image and its radial average over small ranges of wave vector

$q = (4\pi/\lambda)\sin(\theta/2)$ , where  $\lambda$  is the incident laser wavelength and  $\theta$  is the scattering angle.

- Estimate numerically the interaction potential based on the experimentally determined static structure factor  $S(q)$ .

The radial distribution function (Fig. 3) gives the probability to find another particle at a distance  $r$  from the center of a given particle, relative to the probability to find a particle at this distance in an ideal gas [8].

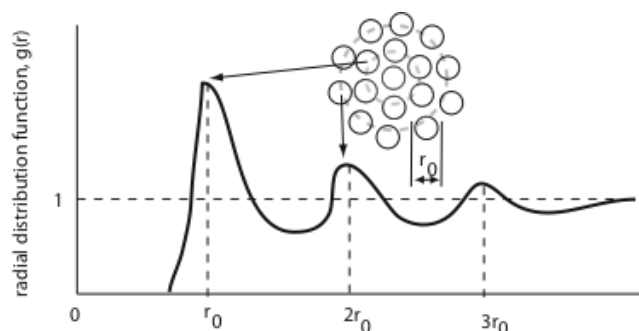


Figure 3. Radial distribution function gives information regarding the intermolecular distances.

The radial correlation function can be computed using experimentally measured static structure factor  $S(q)$ :

$$g(r) = 1 + \frac{1}{2\pi^2 n} \int_0^\infty (S(q) - 1) q^2 \frac{\sin(qr)}{qr} dq \quad (1)$$

The structure factor is very poorly defined for low  $q$  because the azimuthal average of the power spectrum and for this reason is taken over a very limited number of data points. This issue could lead to divergences in  $g(r)$  calculations if the integral in (2) does not tend to zero faster than  $r$ . A possible solution is to set  $g(r)$  to zero below a cutoff wave number  $q$  that is determined by the signal to noise ratio of the experimental  $S(q)$ .

## 4 RESULTS

We computed numerically the integrals in (1) and determined the RDF. Since we worked with images recorded at different times with different resolutions, we present the RDF in arbitrary units (a.u.) The position of the first peak in RDF determines the radius of first coordination shell (Fig. 3), which is proportional to the smallest wave vector  $q_{min}$  of the corresponding experiment.

### 4.1 Small angle light scattering in microgravity experiments on pure fluids

We used a short set almost 600 successive images recorded at 1/25 s frame rate immediately after the pure fluid  $\text{SF}_6$  was quenched below critical temperature. The RDF computed using the static structure factor  $S(q)$  derived from image as described in section 3 shows the characteristic

oscillatory behavior (Fig. 4A) with the coordination shell diameter slightly increasing over time (Fig. 4B). We tested different methods of accounting for the optical background and here we only present the results obtained by filtering the original images with a filter of size 11 pixels.

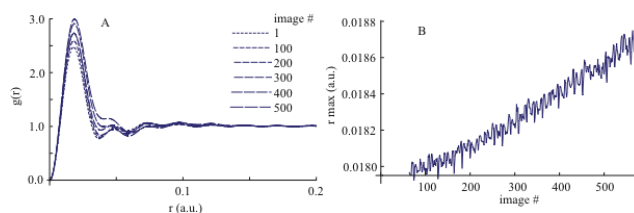


Figure 4. Radial distribution function for  $\text{SF}_6$  in microgravity quenched below critical temperature (A) obtained from the static structure factor. The effective coordination shell has a diameter that slightly increases (B)

The spatial resolution of the images was  $\Delta x = 3.1 \mu\text{m}/\text{pixel}$  and we used square images with  $N = 190$  pixels. The minimum wave vector for the microgravity experiments is, therefore,  $q_{min} = 2\pi/(N \Delta x) = 1 \text{ cm}^{-1}$ . Based on Fig. 4B, the diameter of the effective coordination shell is of the order of  $180 \mu\text{m}$  and slightly increases over time.

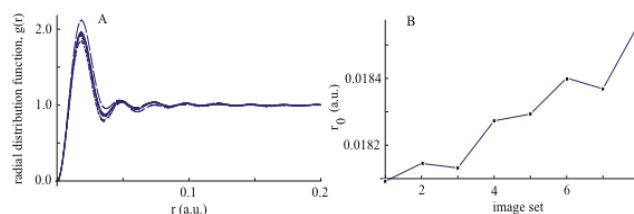


Figure 5. Radial distribution function for  $\text{SF}_6$  in microgravity quenched below critical temperature (A) obtained from the dynamic structure factor. The effective coordination shell has a diameter that slightly increases (B).

The static structure factor requires an optical background in order to correctly account for noise. Dynamical structure factor is computed as detailed in section 3, except the fluctuation image is the difference between the actual image and the average over a large set (in our case 64) of successive images. We plotted only the results regarding every other set of the overlapping sets of images starting with (Fig. 5): 63, 95, 127, 159, 191, 223, 255, 287, 319, 351, 383, 415, 447, 479, 511. Both the static and dynamic structure factor method gave similar values for the coordination distance.

### 4.2 Small angle light scattering from gold nanocolloids on earth

The minimum wave vector for the gold nanocolloids experiments was  $q_{min} = 4.62 \text{ cm}^{-1}$ . Based on Fig. 6B, the diameter of the effective coordination shell is of the order of  $43 \mu\text{m}$  and slightly increases over time.

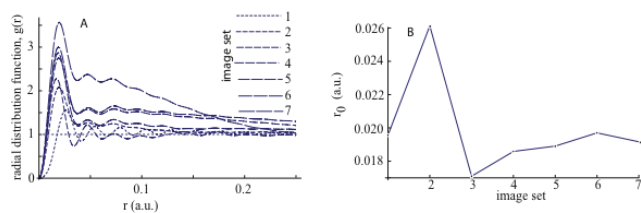


Figure 6. Radial distribution function for gold nanocolloids on earth (A) obtained from the dynamic structure factor. The diameter of the effective coordination shell fluctuates (B).

For nanocolloids, since the concentration fluctuations are very slow and it takes days for the system to become homogeneous, the background was computed over sets of 1000 images. We plotted only the results regarding every other set of the overlapping sets of images (Fig. 6): 1, 3600, 7200, 10800, 14400, 18000, 21600, 28800, 32391, 36000, 39591, 43191, 46791, 72000, 108000, and 144000. At a rate of one frame per second, the RDF in Fig. 4 covers 145000s (over 40 hours) of continuous recording. Shortly after the gradient of concentration was established (see subsection 2.2), the RDF has the expected shape (Fig. 3). However, while the concentration-driven diffusion progresses, the RDF deviates significantly from the two-particle correlation shown in Fig. 3. The reason is that gold nanoparticles form clusters that change RDF.

## 5 CONCLUSIONS

We successfully extracted the RDF by numerically integrating the structure factor obtained from recorded fluctuation images. There is no significant difference between the RDF obtained from the static SF versus dynamic SF. Both pure fluids near critical point in microgravity and nanocolloids on earth showed a slightly increasing coordination distance over time. The phenomenon is due to relaxation towards thermodynamic equilibrium.

## REFERENCES

[1] D. Beysens, J. Straub, D.J. Turner, Phase Transitions and Near-Critical Phenomena, in: H.U. Walter (Ed.) Space, A European Perspective, Springer, Berlin, 1987, pp. 221.  
 [2] Y. Garrabos, B.L. Neindre, P. Guenoun, B. Khalil, D. Beysens, Europhysics Letters, 19 (1992) 491.

[3] F. Croccolo, D. Brogioli, A. Vailati, M. Giglio, D.S. Cannell, Annals of the New York Academy of Sciences, 1077 (2006) 365-379.  
 [4] O. Glatter, O. Kratky, Small Angle X-ray Scattering, Academic Press, 1982.  
 [5] G. Fritz, A. Bergmann, J. Appl. Cryst., 37 (2004) 815-822.  
 [6] A. Szczygielska, A. Burian, S. Duber, J.C. Dore, V. Honkimaki, Journal of Alloys and Compounds, 328 (2001) 231-236.  
 [7] V.A. Loiko, A.P. Ivanov, V.P. Dik, Journal of Applied Spectroscopy, 42 (1985) 571-576.  
 [8] G. Fritz-Popovski, Journal of Chemical Physics, 131 (2009) 114902.  
 [9] A. Oprisan, S.A. Oprisan, J.J. Hegseth, Y. Garrabos, C. Lecoutre-Chabot, D. Beysens, Phys Rev E Stat Nonlin Soft Matter Phys, 77 (2008) 051118.  
 [10] A. Oprisan, S. Oprisan, A. Teklu, Appl. Opt., 49 (2010) 86-98.

## ACKNOWLEDGMENTS

NASA Grants NAG3-1906 and NAG3-2447 to J.J. Hegseth supported Microgravity experiments. Nanocolloids experiments and data analysis was supported by a NASA-SCSGC to A. Oprisan. S.A. Oprisan acknowledges NSF CAREER award IOS-1054914.